Cell Reports, Volume *42*

Supplemental information

Tspan6 stimulates the chemoattractive potential of breast cancer cells for B cells in an EV- and LXR-dependent manner

Guerman Molostvov, Mariam Gachechiladze, Abeer M. Shaaban, Steven Hayward, Isaac Dean, Irundika H.K. Dias, Nahla Badr, Irini Danial, Fiyaz Mohammed, Vera Novitskaya, Liliia Paniushkina, Valerie Speirs, Andrew Hanby, Irina Nazarenko, David R. Withers, Steven van Laere, Heather M. Long, and Fedor Berditchevski

Supplementary Table 1. Related to Figure 1. Percentage of CD14+, CD3+ and CD19+ migrated towards BCa-CM

	SKBr3-CM		MDA-MB-468-CM	
	Healthy donors	BCa patients	Healthy donors	BCa patients
CD14+	10.2-31.8%	3.9-34.3%	2.1-9.4%	2.9-12.4%
CD3+	37.9-57.2%	32.1-60%	49.1-62.5%	40.5-69.9%
CD19+	3.9-13.7%	4.3-16.9%	9.4-22.9%	6-17.1%

	SUM149-CM	MCF7-CM
	Healthy donors	Healthy donors
CD14+	40.7.6-56.8%	12.1-40.2%
CD3+	19.8-51.3%	30.0-79.4%
CD19+	6.1-7.3%	5.9-15.7%

Supplementary Table 2. Related to Figure 1. The concentration of B cell chemokines in media conditioned by breast cancer cells.

Cell line	CXCL13 (pg/ml)	CXCL12 (pg/ml)	CCL20 (pg/ml)	CXCL8 (pg/ml)	CXCL16 (pg/ml)
SUM149	142.7±2.5	666.0±6.6	48.2±5.7	49.2±0.9	253±37.5
MDA-MB-468	135.8±1.6	739.2±12.8	280.6±14.8	54.7±0.6	418.1±29.5
MCF7	136.4±2.9	714.4±12.1	ND*	54.1±0.5	184.4±31.2
SKBr3	47.7±2.5	786.8±15.7	20.1±1.4	48.7±0.3	145.7±7.8

ND* - below the detection level

Supplementary Table 3. Related to figure 4. Expression of tetraspanins in SUM149 cells.

antibodies	**MFIs**
Negative control	360
TSPAN4	1265
TSPAN6	629
TSPAN13	609
Tspan27/CD82	659
Tspan24/CD151	1036
Tspan28/CD81	10240

Expression of Tspan6 in isogenic human BCa cells and mouse mammary carcinoma cells.

Cell line	Negative control, MFI	Positive control, MFI	Expression of Tspan6, MFI
E0771/pLVx	263	9460	298
EO771/Tspan6	399	13989	6588
MDA468/pLVx	57	2908	81
MDA468/Tspan6	75	2810	1964
MDA468/Tspan6-Oxy	85	2930	1875
PY2T/pLVx	295	2252	374
Py2T/Tspan6	308	2627	1549
MCF7/pLVx	417	3240	471
MCF7/Tspan6	419	3259	2359
MCF7/Tspan6-Oxy	422	3190	2275
HCC70/pLVx	223	2975	1067
HCC70/shT6-1	203	2227	238
HCC70/shT6-2	248	3701	282
SKBr3/pLVx	306	9670	373
SKBr3/Tspan6	323	9230	3701

Supplementary figures

Suppl.Fig.1. Related to Figure 1. Migration of B cells towards BCa-CM is not dependent on pertussis toxin (PTX) – sensitive receptors. A. Profiling of chemokines secreted by breast cancer cell lines. Cells were grown for 72 hours and culture supernatants were profiled using Human Chemokine Antibody Array (R&D Systems). **B,C.** Media conditioned MDA-MB-468 cells (**B**) or SUM149 cells (**C**) were used as chemoattractant for human PBMCs purified from healthy donors. PBMCs were pre-treated for 2 hours with PTX (1μg/ml) (or left untreated), and, subsequently, were allowed to migrate for 16-18 hours in the presence (or absence) of PTX. Migrated cells were profiled by flow cytometry. Note, PTX inhibited migration of CD14+ monocytes (left panel) whereas migration of B cells was only marginally affected. Incubation of cells with PTX did not affect the viability of PBMCs (96-98%). **D,E.** Media conditioned MDA-MB-468 cells (**D**) or MCF-7 cells (**E**) were used as chemoattractant for human PBMCs purified from healthy donors. Cells were allowed to migrate for 16-18 hours towards BCa-CM supplemented with various concentrations of anti-midkine mAb. Isotype control mouse mAb were IgG2a. Migrated cells were profiled by flow cytometry. Shown are means and SD from three separate experiments.

A.

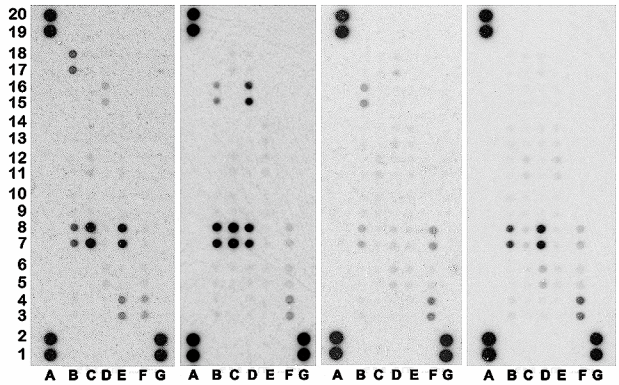

Coordinate	Analyte/control
A1,A2,A19,A20	*Reference spots*
B3,B4	CCL21
B5,B6	CCL28
B7,B8	CXCL16
B9,B10	Chemerin
B11,B12	CXCL5
B13,B14	CCL26
B15,B16	CX3CL1
B17,B18	CXCL1
C3,C4	CCL14
C5,C6	CCL1
C7,C8	CXCL8
C9,C10	IL-16/LCF
C11,C12	CXCL10
C13,C14	CXCL11
C15,C16	Lymphotactin
C17,C18	CCL2
D3,D4,	CCL7
D5,D6	CCL22
D7,D8	Midkine
D9,D10	CXCL9
D11,D12	CCL3,CCL4
D13,D14	CCL15
D15,D16	CCL20
D17,D18	CCL19
E3,E4	CXCL7
E5,E6	CCL18
E7,E8	CXCL4
E9,E10	CCL5
E11,E12	CXCL12
E13,E14	CCL17
E15,E16	CXCL17
F3,F4	Fibrinogen (sample control)
F5,F6	gp130 (sample control)
F7,F8	TfR, CD71
F9,F10	negative control
G1,G2	*Reference spots*

B.

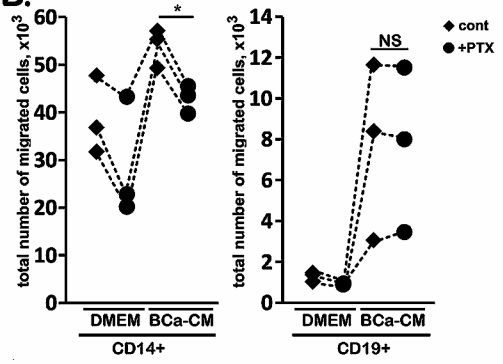

C.

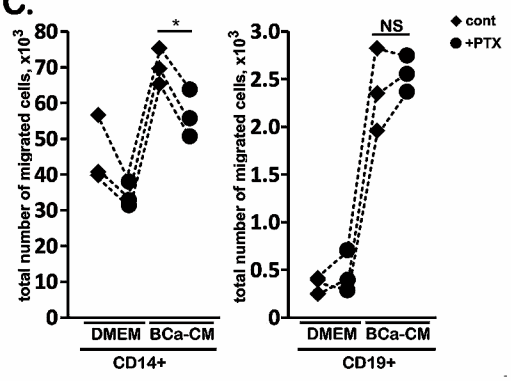

D.

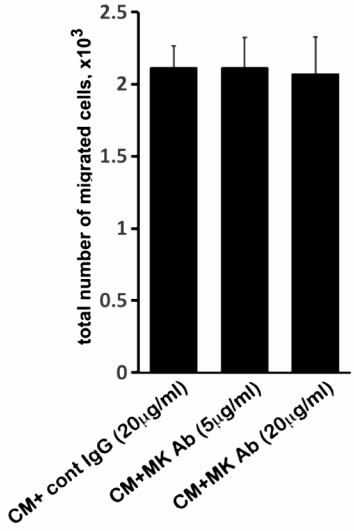

E.

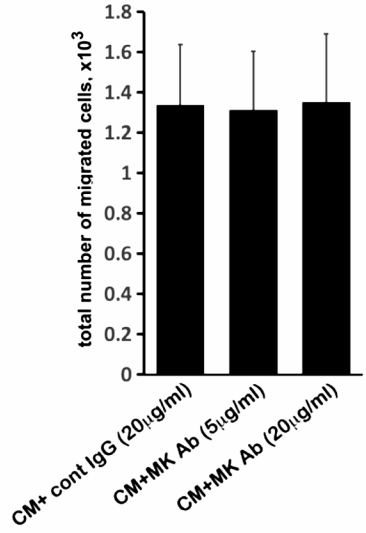

Suppl.Fig.2. Related to Figure 2. Detection of GFP in migrated B cells exposed to GFP-expressing EVs. EVs purified from supernatants conditioned by GFP-expressing human MDA-MB-468 or mouse Py2T cells were added to serum-free media and used as chemoattractants for human PBMCs or mouse splenocytes, respectively. For "control" samples, serum-free media was supplemented with an equal volume of PBS. Cells were allowed 18hrs to migrate and subsequently migrated (M) and non-migrated (NM) cells were profiled for GFP expression by flow cytometry. All plots were pre-gated on CD19+ cells.

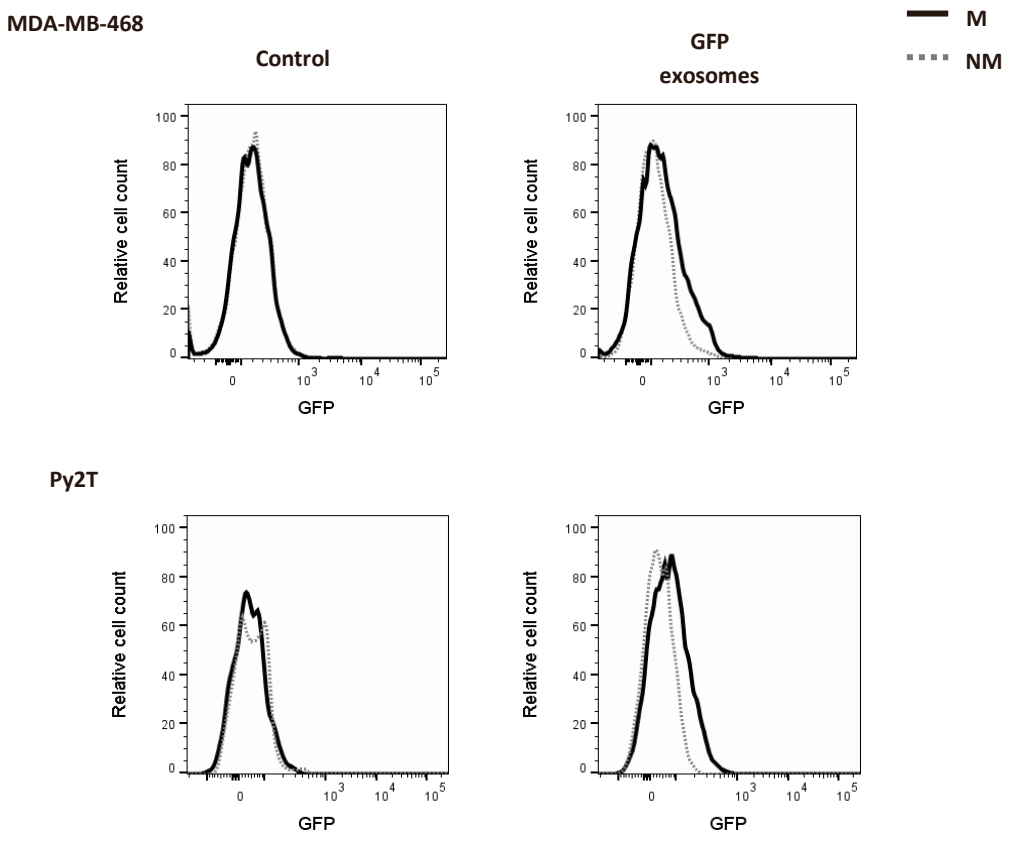

Suppl.Fig.3. Related to Figure 4. Alignment of Tetraspanin transmembrane domains (TM). Inward cavity facing polar residues within tetraspanin TMs are highlighted in red.

TM1

Tspan4	...LMFAFNLLFWLGGCGVLGVGIWL...
Tspan6	...VLLIYTFIFWITGVILLAVGIWG...
Tspan13	...CLCALNLLYTLVSLLLIGIAAWG...
Tspan24/CD151	...LLFTYNCCFWLAGLAVMAVGIWT...
Tspan27/CD82	...FLFLFNLIFFILGAVILGFGVWI...

TM2

Tspan4	...LLIITGAFVMAIGFVGCLGAI...
Tspan6	...VLIATGTVIILLGTFGCFATC...
Tspan13	...VVIAVGIFLFLIALVGLIGAV...
Tspan24/CD151	...ILVVAGTVVMVTGVLGCCATF...
Tspan27/CD82	...VFIGVGAVTMLMGFLGCIGAV...

TM3

Tspan4	...CLLLTFFLLLLLVFLLEATIAILF...
Tspan6	...WMLKLYAMFLTLVFLVELVAAIVG...
Tspan13	...VLLFFYMIILLLVFIVQFSVSCAC...
Tspan24/CD151	...NLLRLYFILLLIIFLLEIIAGILA...
Tspan27/CD82	...CLLGLYFAFLLLILIAQVTAGALF...

TM4

Tspan4	...LLAVGIFGLCTALVQILGLTFAMTM...
Tspan6	...MGVVAGISFGVACFQLIGIFLAYCL...
Tspan13	...LRFVGGIGLFFSFTEILGVWLTYRY...
Tspan24/CD151	...LRVIGAVGIGIACVQVFGMIFTCCL...
Tspan27/CD82	...LGIILGVGVGVAIIELLGMVLSICL

Suppl.Fig.4. Related to Figure 4. Characterisation of expression levels of GFP-tagged tetraspanins in SUM149 cells. Expression of ectopically introduced GFP-tagged tetraspanins in SUM149 cells was assessed by flow cytometry. “T4” – Tspan4; “T6” – Tspan6; “T13” – Tspan13.

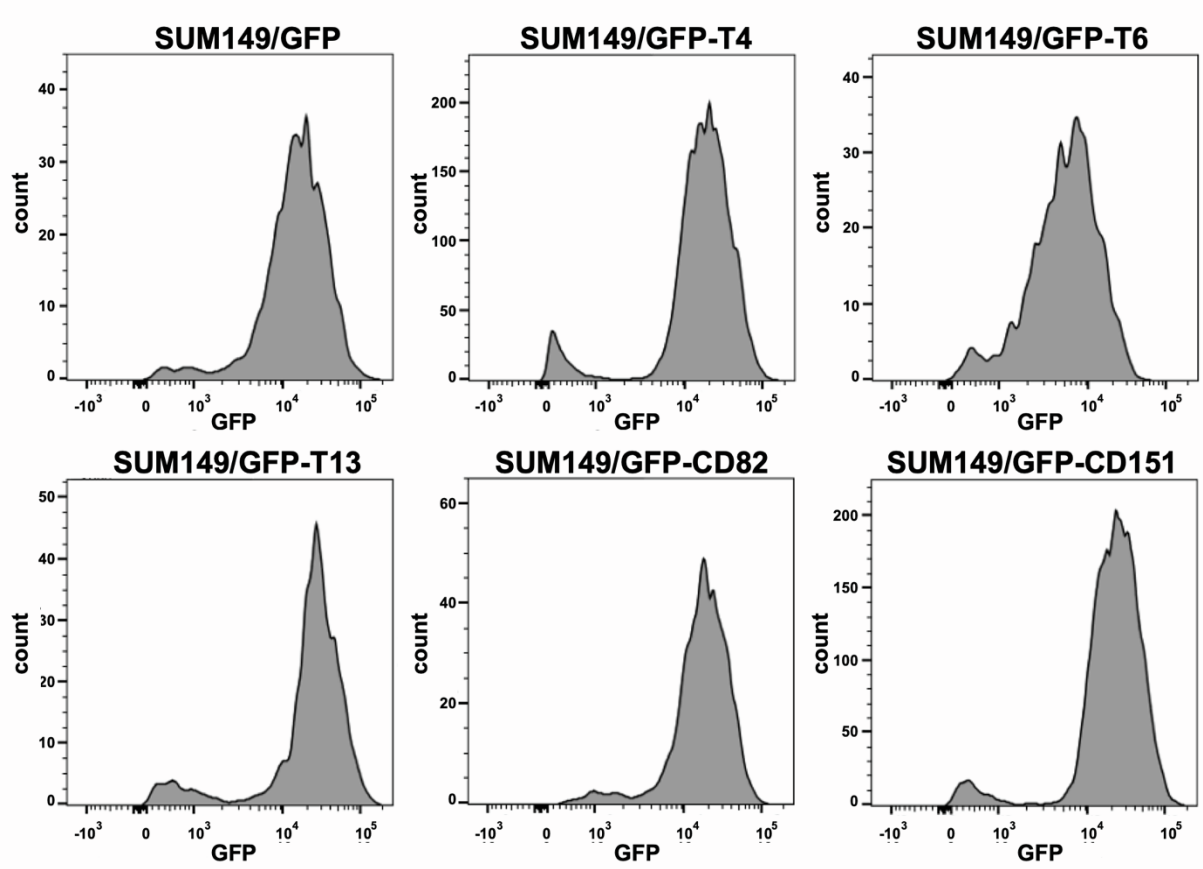

Suppl.Fig.5. Related to Figure 4. Expression of Tspan6 facilitates recruitment of B cells into mouse mammary carcinomas. E0771/pLVx and E0771/Tspan6 cells were injected into mammary fat pads of Kaede mice and tumours were allowed to grow until their size reached approximately 60-80mm^3. Photoconversion of the 'Kaede Green' protein to the converted 'Kaede Red' version was achieved by exposing tumours to UV light. Shown is an example of quantification of the proportion of newly infiltrated (Kaede Green$^+$) B220$^+$ B-cells, CD4$^+$ T cells, and CD8$^+$ T cells 48 hours after tumour photoconversion.

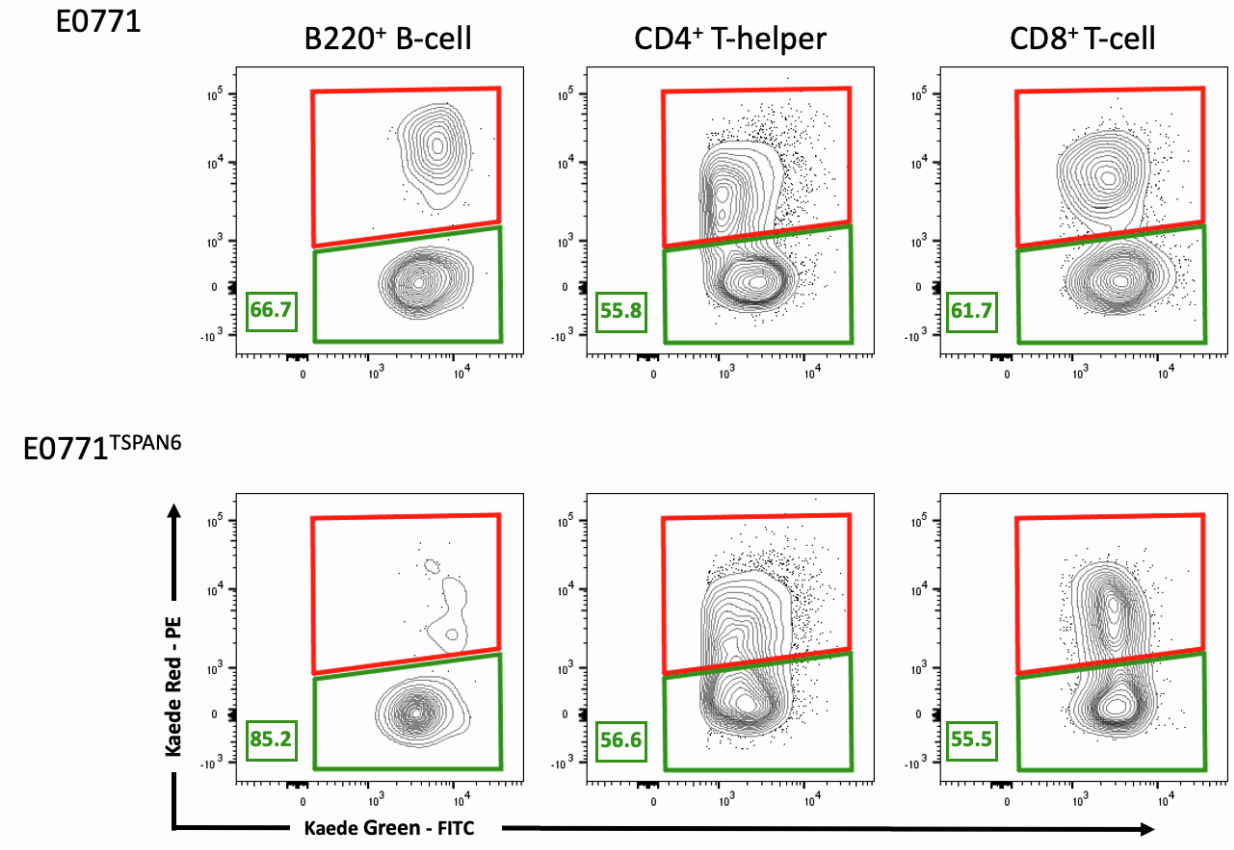

Suppl.Fig.6. Related to Figure 4. Expression of Tspan6 facilitates recruitment of B cells into mouse mammary carcinomas. PY2T/pLVx and PY2T/Tspan6 cells were injected contralaterally into mammary fat pads of 10 FBV mice. Weight of the tumours at day 14.

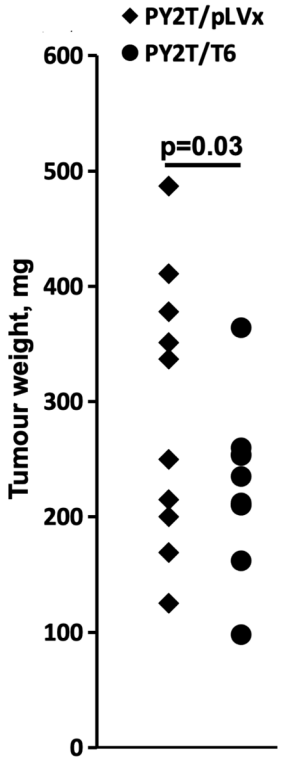

Suppl.Fig.7. Related to Figure 6. The effect of the expression of Tspan6 on the total membrane (A) and cellular levels of 25- and 27-hydroxycholesterols. Total cellular oxysterols were extracted and analysed using LC-MS/MS (25-hydroxycholesterol; 25-HC and 27-hydroxycholesterol; 27-HC). For cholesterol and each of the oxysterols the measurements were normalised as total amounts of lipids per total amounts of cellular proteins measured in three separate experiments.

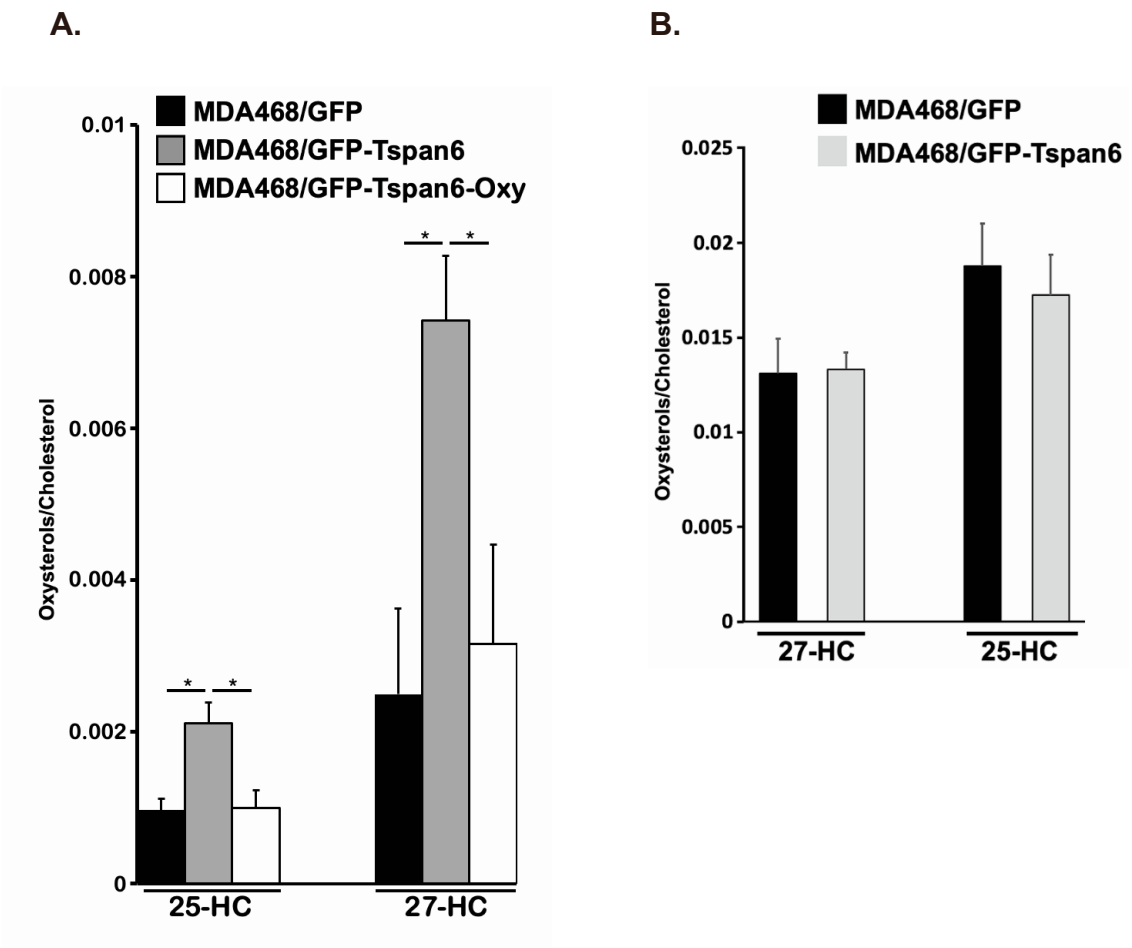

Suppl.Fig.8. Related top Figure 7. Infiltration of CD20+ lymphocytes and expression of Tspan6 in breast cancer tissue microarrays. Examples of CD20 staining (**A**) and Tspan6 immunohistochemical scores (**B**) including positive (scores 3+ and 2+) and negative (score 1+) expression.

A.

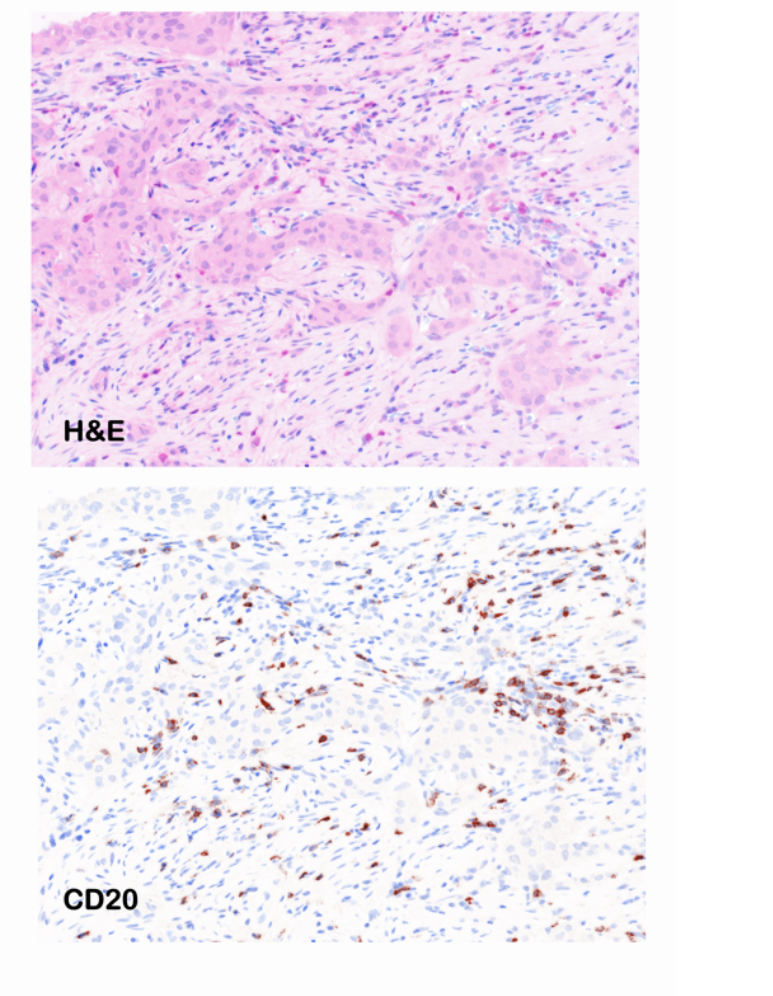

B.

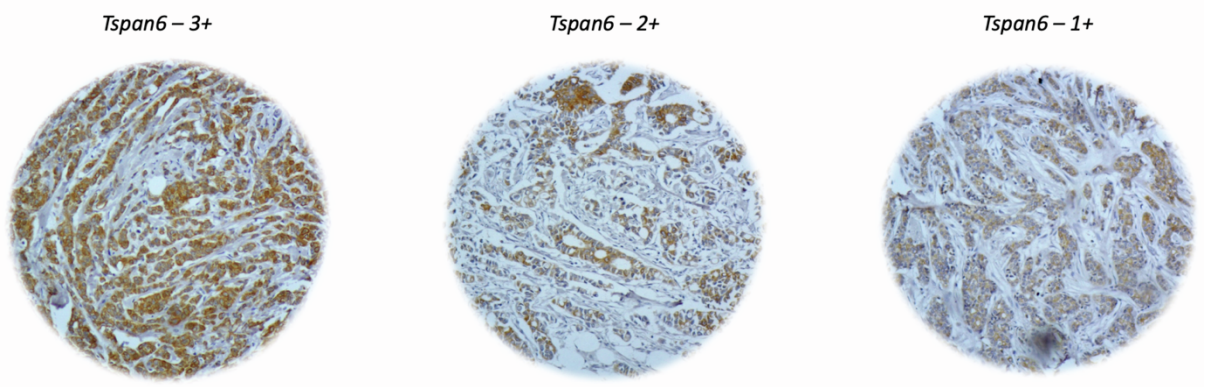

Suppl.Fig.9. Related to Figure 2. Characterisation of EVs purified from MDA-MB-468-CM. A. Cellular and EV lysates were resolved in SDS-PAGE. Proteins were transferred to nitrocellulose membrane and probed with indicated Abs. **B.** NTA analysis of the size of EVs from three independent purification samples (triplicate measurements for each sample). **C.** Transmission electron microscopy of purified EVs.